Phospholipase A_2 Hydrolysis of Mixed Phospholipid Vesicles Formed on Polyelectrolyte Hollow Capsules

Liqin Ge,[a] Helmuth Möhwald,[b] and Junbai Li*[a]

Abstract: Mixtures of the phospholipids L-α-dimyristoylphosphatidic acid (DMPA) and L-α-dipalmitoylphosphatidylcholine (DPPC) have been successfully adsorbed onto the charged surface of multilayer polyelectrolyte capsules to form a novel vesicle. Leaving such vesicles in phospholipase A_2 solution, we observed the hydrolysis reaction on the surface of the lipid/polymer vesicles and a permeability change before and after the reaction by confocal-laser scanning microscopy (CLSM). A capsule with adjustable permeability was constructed. This method may provide new features for drug-release vesicles.

Keywords: enzymes · lipids · microcapsules · permeability · vesicles

Introduction

The formation of multilayers on the nano scale by consecutive deposition of oppositely charged polyelectrolytes onto flat solid substrates has been well developed recently as an assembly technique.[1] The driving force of multilayer assembling is based on electrostatic interaction of the polymer chains. This technology has been successfully applied to the assembly of polyelectrolyte multilayer films on the surface of colloidal particles.[2] Removing of the templating colloidal cores creates a novel route to obtaining hollow polyelectrolyte shells.[2] As a tiny chemical container, the capsule is also used to carry out a chemical reaction.[3] Lipid layers adsorbed onto polyelectrolyte multilayer shells have been considered to provide a seal against small hydrophilic molecules that are otherwise able to penetrate the polyelectrolyte shells.[4]

PLA_2 is a small, stereoselective, calcium-dependent enzyme that hydrolyzes the sn-2 ester linkage of phosphatidylcholine. This has been quantitatively detected by using various techniques like grazing-incidence X-ray diffraction, FTIR spectroscopy, Brewster angle microscopy (BAM), and so on.[5–8] It has been reported that, in unilamellar vesicle solution, addition of phospholipase PLA_2 leads to phospholipid hydrolysis and vesicle destabilization.[9–11] In the present work, we chose the mixed-lipid system, L-α-dimyristoylphosphatidic acid (DMPA), which is less hydrolyzed by PLA_2 but is better suited for attraction to the charged polyelectrolyte by electrostatic interaction, and L-α-dipalmitoylphosphatidylcholine (L-DPPC), which is easily cleaved by PLA_2 (Scheme 1), to cover the capsule surface. By making use of the selectivity of the cleavage reaction we anticipate that there are channels produced on the surface of hollow

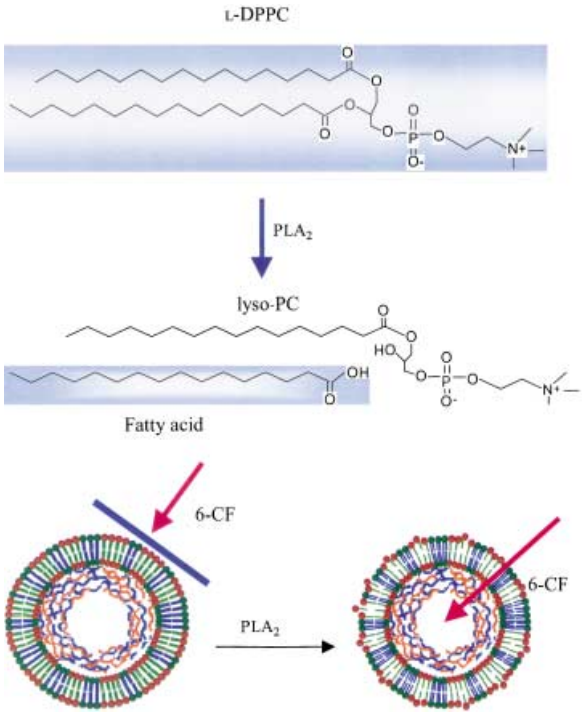

Scheme 1. Schematic description of PLA_2-catalyzed lipid/polymer vesicles.

[a] Prof. Dr. J. Li, Dr. L. Ge
International Joint Lab,
Key Lab of Colloid and Interface Science
The Center for Molecular Science, Institute of Chemistry
Chinese Academy of Science, Beijing 100080 (China)
Fax: (+86) 10-8261-2484
E-mail: jbli@infoc3.icas.ac.cn

[b] Prof. Dr. H. Möhwald
Max-Planck-Institut of Colloids and Interfaces
Am Muehlenberg 2, 14476 Golm/Potsdam (Germany)

 DOI: 10.1002/chem.200304315

polyelectrolyte capsules to enable controlled capsule permeability for drug delivery.

Results and Discussion

Lipid vesicles formed on the surface of capsules: Figure 1a shows CLSM images of multilayer polyelectrolyte capsules coated with fluorescently labeled lipids. The green ring shows the fluorescence intensity of the lipids along the perimeter of the whole capsule surface. Within the resolution of confocal microscopy, a homogeneous capsule with a lipid cover is observed. This demonstrates that mixed phospholipids have been successfully adsorbed onto the surface of the capsules. One can also see that inside the capsule there are some green dyes; this indicates that some labeled lipids also penetrated into the capsules, since the multilayer shell is permeable for small molecules.[3, 12] In order to quantify the change in the fluorescence intensity of the capsule wall, the fluorescence distribution along a line indicated in Figure 1a was recorded. As shown in Figure 1b, from the profile one deduces that the highest fluorescence intensity on the capsule wall is more than 250 units, also that there is some fluorescence in the bulk, which is caused by the unremoved NBD-DPPC and is above the noise level.

Enzymatic reaction of PLA_2 with lipids on the surface of capsules: After the aqueous solution of PLA_2 is added to the solution with lipid-coated capsules, the reaction may take place. Indeed, an intensity decrease of the lipid vesicles on the capsule surface has been observed, Figure 2a. Correspondingly, there will be more cleavage products remaining in the matrix after hydrolysis. Figure 2b shows the decreased fluorescence-intensity distribution on the capsule wall after five hours' reaction time. The highest fluorescence intensity from the wall is reduced by an order of magnitude, and from this can be inferred that the fluorescence intensity decreased dramatically because of the PLA_2-catalyzed phospholipid

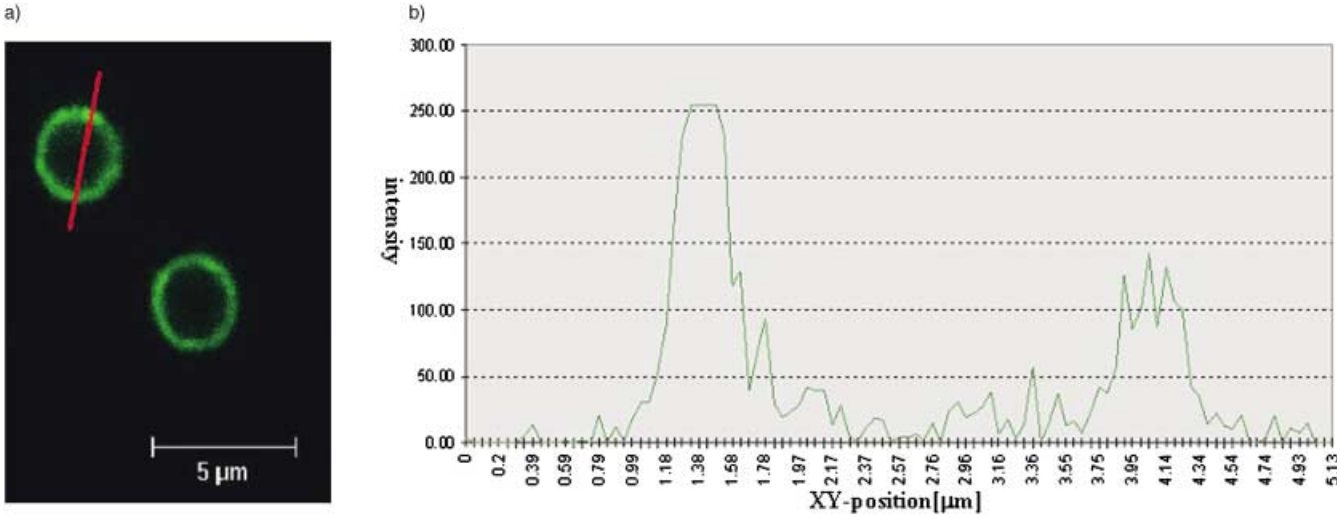

Figure 1. a) CLSM image of a multilayer polyelectrolyte capsule covered by mixed lipids (DMPA/DPPC/NBD-DPPC 30:60:10, *w*/*w*); b) The profile diagram of the fluorescence intensity along the red line.

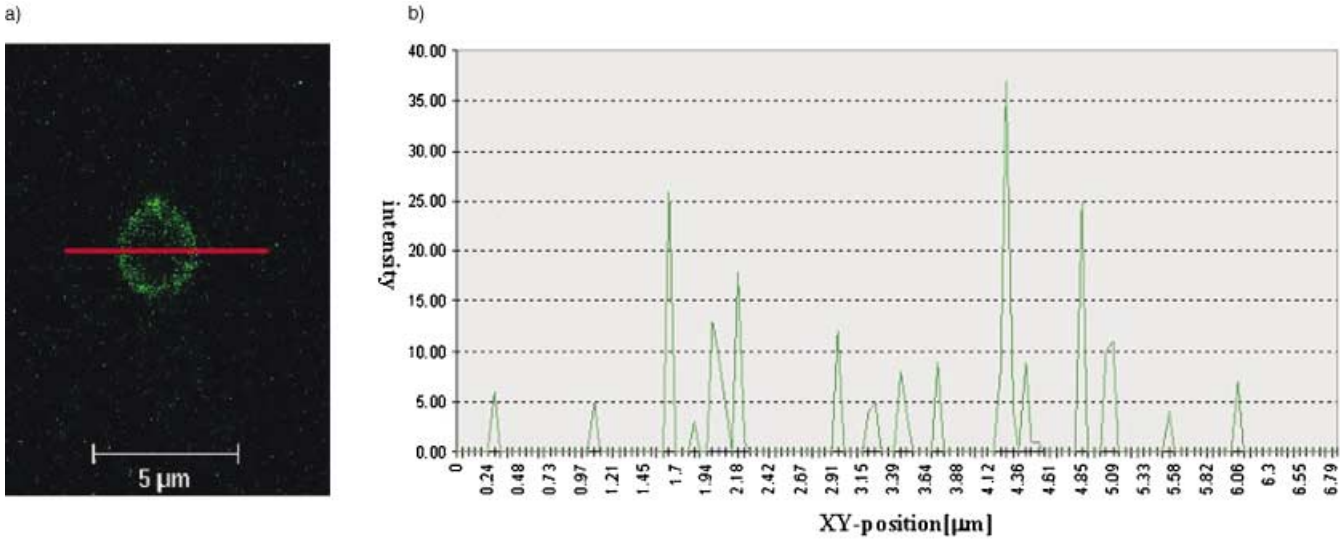

Figure 2. a) CLSM image of PLA_2 added to the lipid-coated capsules after 5 hours. b) Profile of the fluorescence intensity along the red line.

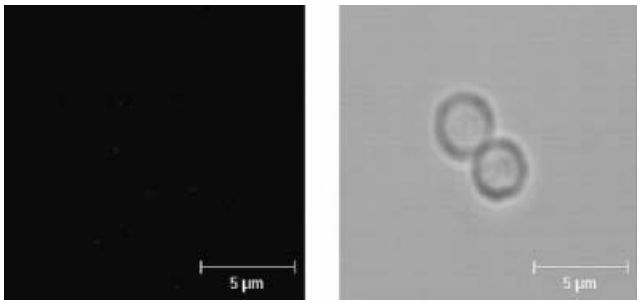

Figure 3. CLSM images of the lipid covered capsules after complete PLA_2 hydrolysis.

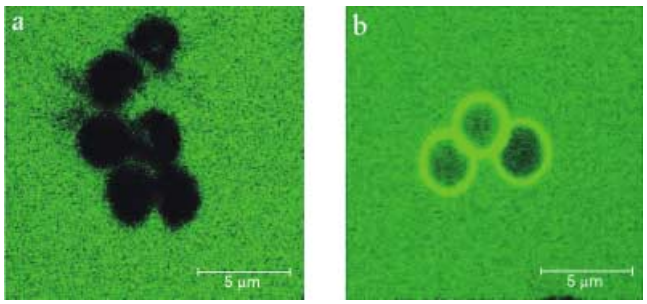

Figure 5. a) CLSM image of lipid-covered multilayer polyelectrolyte capsules in a solution containing the dye 6-CF. The darker center represents the impermeability for dyes through the wall of capsules. b) CLSM image with a partly PLA_2-catalyzed capsule. The dye molecules can penetrate into the capsule, but the dye concentration inside is lower than that outside.

cleavage. After 12 hours, the reaction solution was washed with water by centrifugation, PLA_2 and the hydrolysis products were removed. The absence of fluorescence in Figure 3 (left) indicates that the lipids have been removed. However, judged from measurements of the transmission image in Figure 3 (right), the hollow capsule still remains. This means that the L-DPPC was cleaved by PLA_2 and the surface of the capsules was not coated.

In our hydrolysis system, the phospholipase A_2 buffer solution contains 5 mM Ca^{2+}. It may bind to DMPA and convert it into a quasicrystalline gel phase.[9] This will thus cause a phase separation and lipid layer leaking. To prove this we performed a control experiment by adding a solution of $CaCl_2$ without PLA_2 to the lipid-covered capsule dispersion. Figure 4a and b shows that there is no fluorescence intensity decrease after the lipid-covered capsules were immersed into the $CaCl_2$ solution for 24 hours. Therefore this demonstrates that the observed fluorescence intensity change is indeed due to the PLA_2 hydrolysis.

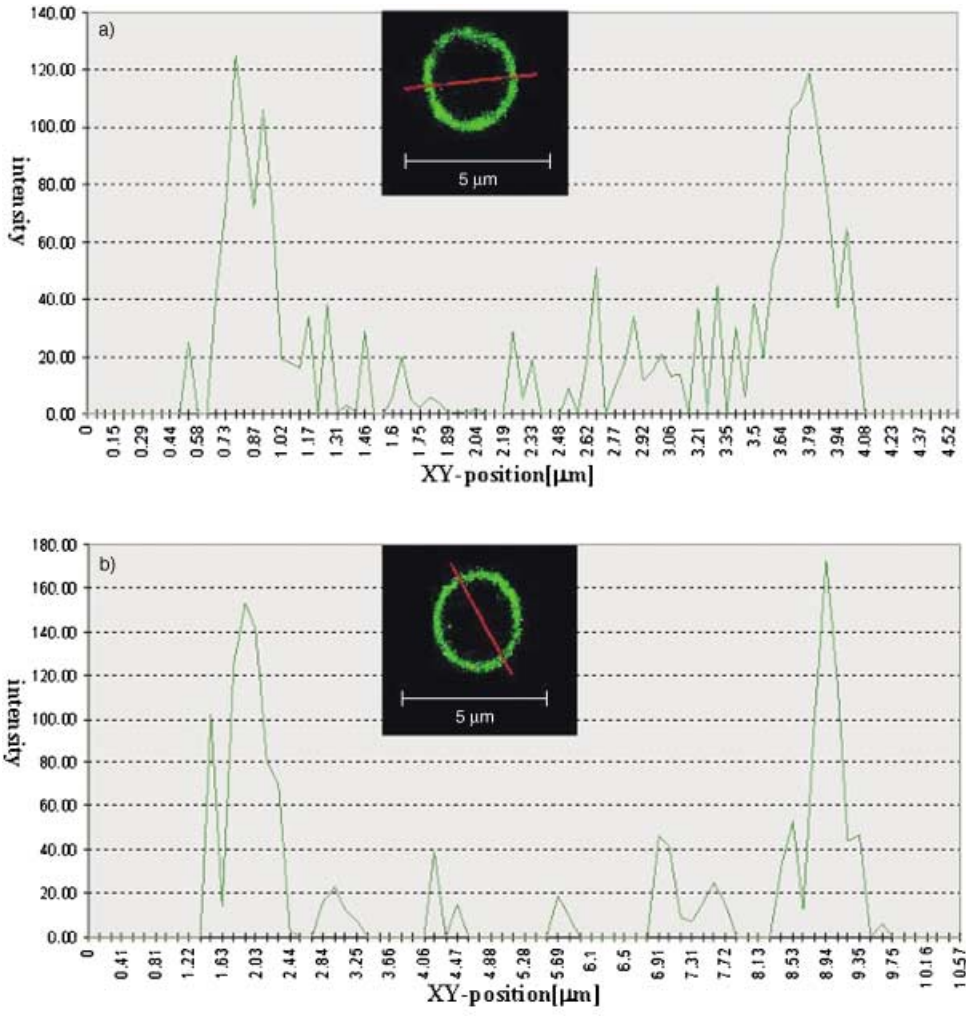

Figure 4. a) CLSM image of a lipid-covered capsule in the $CaCl_2$-containing buffer solution without phospholipase A_2, and profile of the fluorescence intensity. b) Time-dependent CLSM image of the above capsule after 24 hours, and profile of the fluorescence intensity.

Permeability of lipid-covered capsules: The dye 6-CF was used as a probe to study the permeability of capsules with and without coverage of lipids. For this we added 6-CF to the mixed-lipid-covered capsules, then we studied the permeability of 6-CF through the capsule wall by fluorescence microscopy. The image in Figure 5a shows dark spots inside the capsules; this indicates that the small dye molecules 6-CF have been blocked outside the walls of the polyelectrolyte shells. As lipid layers deposited on the surface of capsules they may form unilamellar or bilayer structures. This is why one can only see the dye distribution outside the capsules. After using PLA_2 to cleave the lipid coat, we observed that the dye molecules entered the capsules, as shown in Figure 5b. However, the dye concentration outside is much higher than that inside. This means that the dye penetration into the capsule through the walls takes some time. After 10 minutes one

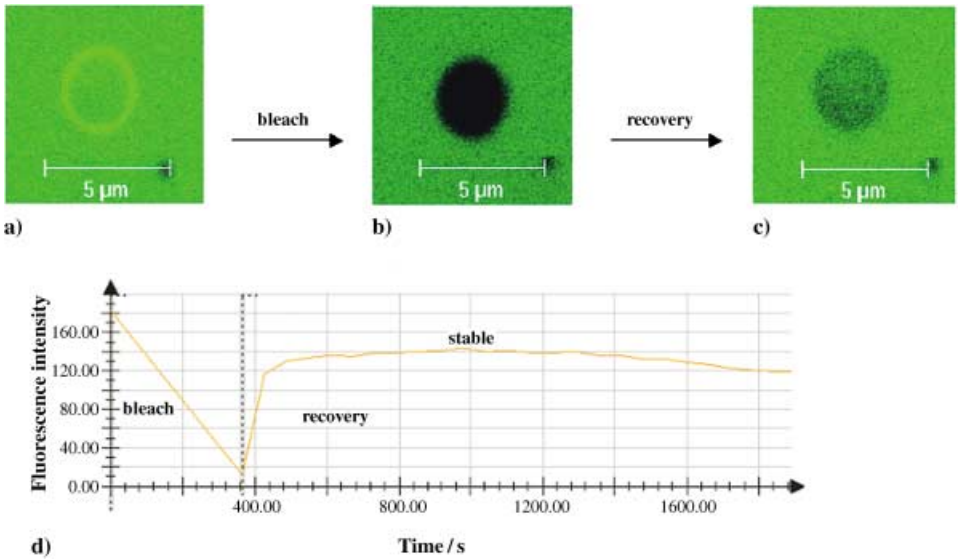

Figure 6. CLSM images of a) capsules mixed with 6-CF dyes before bleaching; b) after bleaching inside the capsule; c) fluorescence recovery; d) intensity profile after bleaching and recovery.

finds a similar fluorescence intensity of dyes inside and outside the capsule, as shown in Figure 6a. To further quantify the penetration of the dye across the wall of the capsule photochemical bleaching experiments were performed as shown in Scheme 2. For quantitative measurements, the fluorescence intensity was integrated by tracing a closed area in the interior (ROI analysis provided by the CLSM software). An Ar ion laser from the CLS microscope with an emission wavelength of 488 nm was focused onto a spot inside the ring of the capsule with maximum power for bleaching. As one can see, most of the dye molecules have lost their fluorescence activity. A dark center inside the capsule can be visualized as shown in Figure 6b.

After a long enough time, almost all of the dye molecules in the capsule had been bleached. Afterwards, we measured the recovery of the fluorescence intensity inside the capsules and recorded the intensity recovery as a function of time (Figure 6d). The CLSM images were taken every 120 seconds during the recovery. Figure 6c shows that 440 s after bleaching the dye molecules are diffusing from outside into the capsules, as quantified by the green fluorescence intensity. From the recovery time ($t \approx 40$ s) one may estimate the diffusion coefficient D. Assuming the transport is diffusive across the wall of thickness $d \sim 22$ nm one obtains:

$$D = \tfrac{1}{2}(22\ \text{nm})^2/40\ \text{s} = 0.55 \times 10^{-13}\ \text{cm}^2\text{s}^{-1}$$

This value is about an order of magnitude lower than values measured for the diffusion of dyes across polyelectrolyte multilayer capsules. It indicates that there may be some sealing of holes in the polyelectrolyte by products of the reaction that have not been removed.

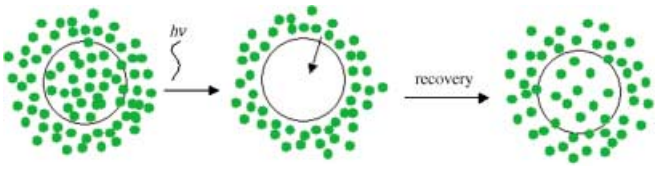

Scheme 2. Scheme of photochemical bleaching and recovery.

Confocal-laser Raman spectra measurements, given in Figure 7, show the evident decreases of the Raman intensity for the two groups, C–O and C–O–C stretch vibrations at 1032 and 1115 cm^{-1}, respectively, after hydrolysis.[13, 14] These two groups exist mainly in the hydrolytic product lyso-PC and the substrate. However at 760 cm^{-1} the PO_2^- diester symmetric stretch vibration did not display a dramatic change.[13, 14] This reflects the fact that the PO_2^- groups remain constant before and after the hydrolysis reaction. All of these results reveal that one of the products, lyso-PC, and some substrates still remained on the surface of the capsules. We have to point out that no special –COOH stretch peak at 1750 cm^{-1} of another product, fatty acid, was observed. This should be ascribed to the fact that this compound has been removed after washing by centrifugation. The above spectroscopic analysis further demonstrates that the lipid hydrolysis reaction by PLA_2 occurred.

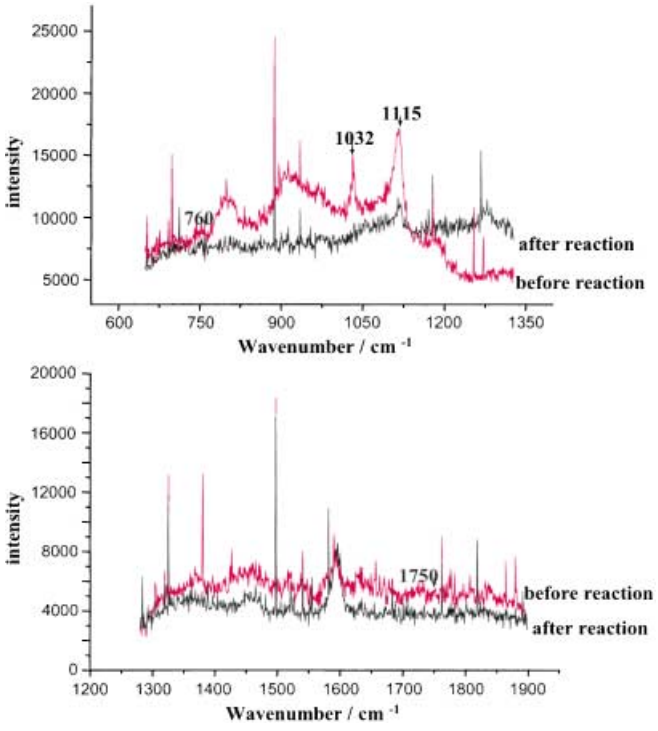

Figure 7. Confocal-laser Raman spectra from 600–1350 cm^{-1} of the mixed DMPA/DPPC lipid covered capsules before and after the hydrolysis reaction by PLA_2 at room temperature. Top: C–O/C–O–C stretch region; bottom: –COOH stretch region.

Surface-morphology change of lipid-covered capsules before and after enzyme cleavage: High-resolution surface force microscopy (HRSFM) is able to provide information by inspecting the capsule wall surface on the nano scale. The surface texture change before and after cleavage of the lipids by PLA_2 was recorded by HRSFM. Figure 8a and b shows the wall texture selected from the inner capsule coating with mixed phospholipids before and after the PLA_2 enzymatic reaction, respectively. After PLA_2 catalyzed the lipid cleavage on the capsule surface, domains can be observed where the permeability of the capsules may be enhanced. The mean roughness before the reaction was calculated to be 4.27 nm, while after the reaction it was 5.06 nm; this means that after the reaction the surface roughness is increased. We cannot yet comment on whether pores have been created by the reaction or if the roughness reappears after removal of the lipid coat.

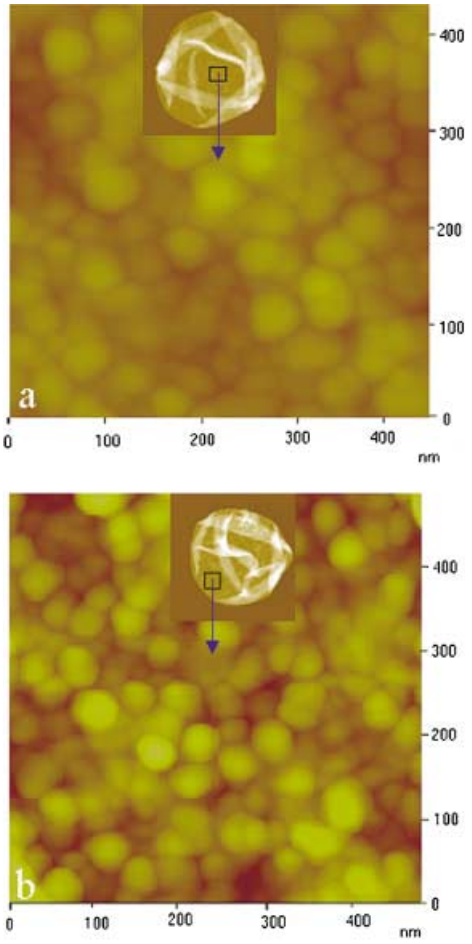

Figure 8. High-resolution scanning force microscopy (contact mode) top view image of the surface texture for lipid/polymer vesicle a) before and b) after hydrolysis by PLA_2.

Conclusion

Mixed phospholipid vesicles have been successfully fabricated on the surface of polyelectrolyte hollow capsules. This design allows one to control the formation of the lipid/polymer capsule to a predetermined size. The enzymatic reaction occurring at the surface alters the permeability of the capsule, which may lend the capsule new features, for example, release triggered by an enzymatic reaction or a highly asymmetric membrane. The triggered influx of the hydrophobic molecules could thus be studied by confocal fluorescence microscopy. This procedure can be applied to biomimetic cells to study the reactions in a living system.

Experimental Section

Materials: Poly(sodium styrenesulfonate) (PSS, $M_w \approx 70\,000\ g\,mol^{-1}$) and poly(allylamine hydrochloride) (PAH, $M_w \approx 70\,000\ g\,mol^{-1}$) were purchased from Aldrich, and L-α-dimyristoylphosphatidic acid (DMPA), L-α-dipalmitoylphosphatidylcholine (L-DPPC), fluorescently labeled l-phosphatidylcholine NBD-(aminohexanoyl)-palmitoyl (NBD-DPPC), 6-carboxyfluorescein (6-CF), and phospholipase A_2 (PLA_2) were purchased

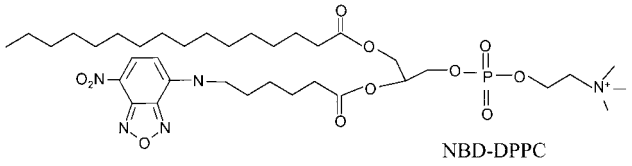

from Sigma. All were used without further purification. The buffer solution for PLA_2 was an aqueous solution containing NaCl (15 mmol), $CaCl_2$ (5 mmol), and tris(hydroxymethyl)aminomethane (10 mmol). Positively charged melamine formaldehyde (MF) particles with a diameter of 2.85 ± 0.09 μm were used as a template for preparing the hollow capsule and were provided by Microparticles GmbH, Berlin.

The concentration of PLA_2 is 20 units per 254 mL. The water used in all experiments was Millipore filtered. All experiments were performed at room temperature.

Preparation of hollow polyelectrolyte shells and of mixed lipid solution: Multilayer assembly was accomplished by adsorption of polyelectrolytes onto MF particles ($1\ mg\,mL^{-1}$). Oppositely charged polyelectrolyte species were subsequently added to the suspension followed by repeated centrifugation. After the expected layers were absorbed, we used hydrochloric acid solution (0.1 mol) to remove the core and obtained hollow polyelectrolyte shells.[12] PSS was used to form the first layer. After alternating adsorption five times, PAH remained as the outermost layer, which has a positive charge and favors negatively charged phospholipid adsorption in a next step.

Mixed phospholipids (DMPA/DPPC/NBD-DPPC 30:60:10, *w*/*w*) were dissolved in a mixed solvent ($CHCl_3$/MeOH 1:1, *v*/*v*, $0.5\ mg\,mL^{-1}$). The mixed-lipid solution obtained was added to the polyelectrolyte shell dispersion to allow adsorption on polyelectrolytes. After 30 minutes, we washed the system three times with water by centrifugation and obtained hollow capsules covered by the lipids.

Confocal-laser scanning microscopy measurements (CLSM): The CLSM images of the capsules were obtained by means of a Leica confocal scanning system. A 100× oil immersion objective with a numerical aperture of 1.4 was used. In this experiment, we chose fluorescently labeled DPPC (L-phosphatidylcholine (NBD-aminohexanoyl)-palmitoyl; 10% *w*/*w*) and 6-CF as fluorescent dyes for visualization. The optical parameters of the CLSM were not changed before and after the enzymatic reaction, hence the measured intensities can be compared quantitatively.

Confocal-laser Raman spectra (CLRS) measurements: Raman spectra were taken at room temperature by using a Confocal Raman Microscope (CRM200, Witec) equipped with a piezo scanner (P-500, Physik Instrumente) and high NA microscope objects (60,NA = 0.80, Nikon). In a typical experiment, circularly polarized laser light (diode-pumped Green laser, 532 nm, CrystaLaser) was focused on the located material with diffraction-limited spot size. The spectra were taken with an air-cooled charge-coupled

device (PI-MAX, Princeton Instruments) behind a grating spectrograph (Acton, 600 g mm) with a high resolution of 6 cm^{-1}.

Scanning-force-microscopy (SFM) measurements: SFM images were recorded at room temperature by using a Nanoscope III Multimode apparatus (Digital Instrument Inc., Santa Barbara, CA). Silicon nitride (Si_3N_4) cantilevers with a force constant of 0.58 $N m^{-1}$ (Digital Instrument) were used for contact SFM. Silicon tips (Olympus and Nanotips, DI) with a resonance frequency of ~300 kHz and a spring constant of ~40 $N m^{-1}$ were employed for tapping-mode SFM imaging. The contact force between the tip and the sample was kept as low as possible (< 10 nN), and images were acquired in constant-force mode (height mode) at a scan rate of 0.5–1 Hz. The samples were prepared by applying a drop of the capsule solution onto freshly cleaved mica or onto glass coverslips. Images were sampled from different areas. SFM images were processed by using Nanoscope software and Image PC software (Version beta 2, Scion Corp.).

Acknowledgement

We acknowledge financial support from the National Nature Science Foundation of China (NNSFC 29925307 and NNSFC 90206035), the Major State Basic Research Development Program (973, Grant. No. G2000078103) as well as the research contract between the German Max Planck Society and the Chinese Academy of Sciences. The authors also thank Anne Heilig for SFM measurements and Wenfei Dong for confocal Raman spectroscopy measurements.

[1] a) G. Decher, J. D. Hong, *Macromol. Chem. Macromol. Symp.* **1991**, *46*, 321–327; b) G. Decher, *Science* **1997**, *277*, 1232–1237.

[2] a) F. Caruso, R. A. Caruso, H. Möhwald, *Science* **1998**, *282*, 1111–1114; b) E. Donath, G. B. Sukhorukov, F. Caruso, S. A. Davis, H. Möhwald, *Angew. Chem.* **1998**, *110*, 2323–2327; *Angew. Chem. Int. Ed.* **1998**, *37*, 2201–2205.

[3] a) L. Daehne, S. Leporatti, E. Donath, H. Möhwald, *J. Am. Chem. Soc.* **2001**, *123*, 5431–5436; d) G. B. Sukhorukov, E. Donath, S. Moya, A. S. Susha, A. Voigt, J. Hartmann, H. Möhwald, *J. Microencapsulation* **2000**, *17*, 177–185.

[4] S. Moya, E. Donath, G. B. Sukhorukov, M. Auch, H. Baeumler, H. Lichtenfeld, H. Möhwald, *Macromolecules* **2000**, *33*, 4538–4544.

[5] a) J. B. Li, J. Z. Chen, X. L. Wang, G. Brezesinski, H. Möhwald, *Angew. Chem.* **2000**, *112*, 3187–3191; *Angew. Chem. Int. Ed.* **2000**, *39*, 3059–3062; b) U. Dahmen-Levison, G. Brezesinski, H. Möhwald, *Prog. Colloid Polym. Sci.* **1998**, *110*, 269–274.

[6] D. W. Grainger, A. Reichert, H. Ringsdorf, C. Salesse, D. E. Davies, J. B. Lloyd, *Biochim. Biophys. Acta* **1990**, *1022*, 146–154.

[7] G. Scherphof, B. V. Leeuwen, J. Wilschut, J. Damen, *Biochim. Biophys. Acta.* **1983**, *732*, 595–599.

[8] M. K. Jain, D V. Jahagirdar, *Biochim. Biophys. Acta.* **1985**, *814*, 313–318.

[9] a) C. R. Kensil, E. A. Dennis, *J. Biol. Chem.* **1979**, *254*, 5843–5848; b) Y. Higashino, A. Matrui, K. Ohki, *J. Biochem*. **2001**, *130*, 393–397.

[10] A. Susana, L. A. Sanchez, E. G. Bagatolli, L. H. T. Theodore, *Biophys. J.* **2002**, *82*, 2232–2242.

[11] R. Wick, M. I. Angelova, P. Walde, P. L. Luisi, *Chem. Biol.* **1996**, *3*, 105–111.

[12] G. B. Sukhorukov, M. Brumen, E. Donath, H. Möhwald, *J. Phys. Chem. B* **1999**, *103*, 6434–6440.

[13] S. F. Parker, *Applications of Infrared, Raman, and Resonance Raman Spectroscopy in Biochemistry*, Plenum, New York, p. 421–479.

[14] T. T. Anthony, *Raman Spectroscopy in Biology: Principles and Applications*, Wiley-Interscience, pp. 187–479.

Received: August 5, 2002
Revised: March 7th, 2003 [F4315]